ISSN 0036-0244, Russian Journal of Physical Chemistry A, 2022, Vol. 96, Suppl. 1, pp. S105–S112. © Pleiades Publishing, Ltd., 2022.

PHYSICAL CHEMISTRY OF NANOCLUSTERS AND NANOMATERIALS

Molecular Modeling of Biofuel Cells of BN Nanotube-FAD Structure

Fatemeh Mollaamin[a,*], Fatma Kandemirli[a], Nayer T. Mohammadian[b], and Majid Monajjemi[a]

[a] *Department of Biomedical Engineering, Faculty of Engineering and Architecture, Kastamonu University, Kastamonu, Turkey*

[b] *Department of Chemistry, Ardabil Branch, Islamic Azad University, Ardabil, Iran*

** e-mail: smollaamin@gmail.com*

Received April 9, 2021; revised May 7, 2021; accepted May 8, 2021

Abstract—Boron nitride nanotube (BNNT) joint to Flavin adenine dinucleotide (FAD) makes a nano-biofuel cell due to the direct electron transfer principle which has been studied by density functional theory methods. Flavin adenine dinucleotide was immobilized on the boron nitride nanotube by linking a simulation water medium. In this work, it has been done the quantum chemical and computational methods to estimate the effect of boron nitride nanotube through electron charge transfer, electric properties including resistance, voltage, and current, conductivity, limiting conductivity, power and nuclear magnetic resonance parameters and thermochemical properties using a Nano-biofuel cell. The results of boron nitride nanotube can be used for generating electric power in lower resistances with the best agreement in linear correlation of voltage-current directly from sustainable fuel substrate such as Flavin adenine dinucleotide (FAD). In this investigation, the data explained that the feasibility of using boron nitride nanotube and Flavin adenine dinucleotide becomes the norm in electrochemical bio system applications.

Keywords: boron nitride nanotube, Flavin adenine dinucleotide, biofuel cell, density functional theory, limiting conductivity, voltage–current, power

DOI: 10.1134/S0036024422140163

INTRODUCTION

The connection between biology and electricity has been known since the experiments of Galvani in the 1780s, nowadays biofuel cells have a key role for study about this connection. Biofuel cells use biocatalysts for the conversion of chemical energy to electrical energy [1].

Biofuel cells consist of a two electrode set (of any stable and electrically conducting material) modified by biocatalytic enzymes to specifically oxidize/reduce substrates [2].

Biofuel cells, in which either enzymes or whole cell organisms are used as the catalyst, have attracted much attention for generating electric power directly from sustainable fuel substrates such as glucose and ethanol. Numerous enzyme fuel cells employing glucose oxidizing enzyme have been reported [3, 4].

Electron transfer has been gotten for many enzymes by immobilizing them within thin films of various sorts on an electrode [5–9]. Glucose oxidase (GOX) based glucose oxidizing electrodes have attracted attention as candidate for bio catalytic fuel cell anodes. The $FAD/FADH_2$ redox cofactor of GOX has a sufficiently negative formal potential for a biofuel cell anode [10]. The resulting anodes operate at potentials significantly more positive than that of $FAD/FADH_2$ and decrease cell voltage output of the biofuel cell [11–14].

p-Hydroxybenzoate hydroxylase catalyzes the oxygenation of *p*-hydroxybenzoate (*p*OHB) to 3,4-dihyroxybenzoate (3,4-diOHB); FAD, NADPH, and molecular oxygen are all necessary for this reaction. NADPH first transfers a hydride equivalent to FAD, creating $FADH^-$, and then $NADP^+$ dissociates from the enzyme. Reduced PHBH then reacts with molecular oxygen to form the flavin-C(4a)-hydroperoxide. The flavin hydroperoxide quickly hydroxylates *p*OHB, and then eliminates water to reproduce oxidized flavin (Scheme 1) [15].

Single walled carbon nanotube can be used to electrically connect glucose oxidase to electrodes to demonstrate direct ET and bio catalysis using functionalized SWCNTs on gold, with FAD [18, 19]. CNTs on other conductive surfaces were also used to obtain direct ET for GOX [20–23].

The most obvious target for biofuel cells research is still for in vivo applications where the fuel used could be withdrawn virtually without limit from the flow of blood to provide a long-term or even permanent power supply for such devices as pacemakers glucose sensors for diabetics ex vivo applications are gastrobat, battery packs for laptop computers and mobile telephones [24].

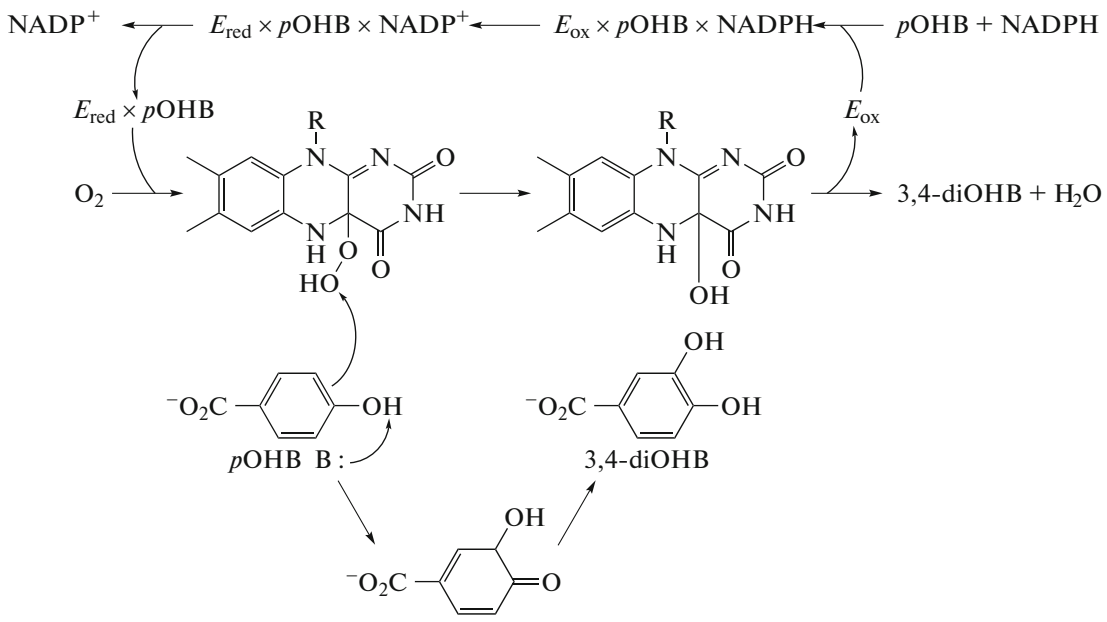

Scheme 1. An alternative flavin-mediated oxygenation mechanism involves the use of a flavin-N(5)-oxide rather than a flavin-C(4a)-(hydro)peroxide [16, 17].

Carbon nanotubes have also been intensively explored to develop optical based sensing approaches for biological in vitro and in vivo molecular sensing and imaging applications in recent years due to their unique properties [25–28].

Among carbon nanotubes, the group III nitrides and especially boron nitride nanotube (BNNT), which always exhibit semi conducting behavior, are considered as proper alternates of CNTs [29, 30]. This behavior and also the equality of total B and N atomic number, which are the first neighbors of C in the periodic table to that of two C atoms, made BNNT as interesting subject of numerous studies [31, 32].

Electron transfer to or from the bio catalytic active sites can be mediated by polymer bound or entrapped redox complexes [33]. In this study we selected flavin adenine dinucleotide (FAD) as a bio catalytic and single walled boron nitride nanotube (SWBNNT) as a entrapped redox complexes.

An enzyme fuel cell using a carbon electrode and bacterial FAD dependent glucose dehydrogenase (FADGDH) based on the direct electron transfer principle was constructed which its scalability and cellulolytic sugar conversion were studied [34–36].

Since the discovery of carbon nanotube in 1991 nanotubes have received much attention, BNNT together with carbon nanotube are considerate to be promising material for the electronic industry due to their structure and physical properties [37, 38].

FAD is a redox cofactor involved in several important reactions in metabolism. Many oxidoreductase called falvoenzyme or flavor proteins, required fad as a prosthetics group, which function in electron transfer.

In electrolytes, electrical conduction happens not by band electrons or holes, but by full atomic species (ions) traveling, each carrying an electrical charge. The resistivity of ionic liquids varies tremendously by the concentration, while distilled water is almost an insulator; salt water is a very efficient electrical conductor [39–41].

Electrolyte solutions can also result from the dissolution of some biological and synthetic polymers, termed polyelectrolytes, which contain charged functional groups.

In this paper, we have recombinantly prepared FAD to construct a boron nitride nanotube (BNNT) based direct electron transfer type enzyme fuel cell, and investigated its stability, residence, nuclear magnetic resonance parameters and electrochemical properties [42, 43].

THEORETICAL BACKGROUND AND COMPUTATIONAL METHOD

One of the most employed approximations is the Hartree–Fock "self-consistent field" approximation and DFT methods. The density-functional theory of Hohenberg, Kohn, and Sham allow for the theoretical study of material properties [44].

DFT theory proves an advantageous method for predicting chemical systems, and in order to understand its similarities and differences to other computational methods employed, a brief introduction dealing

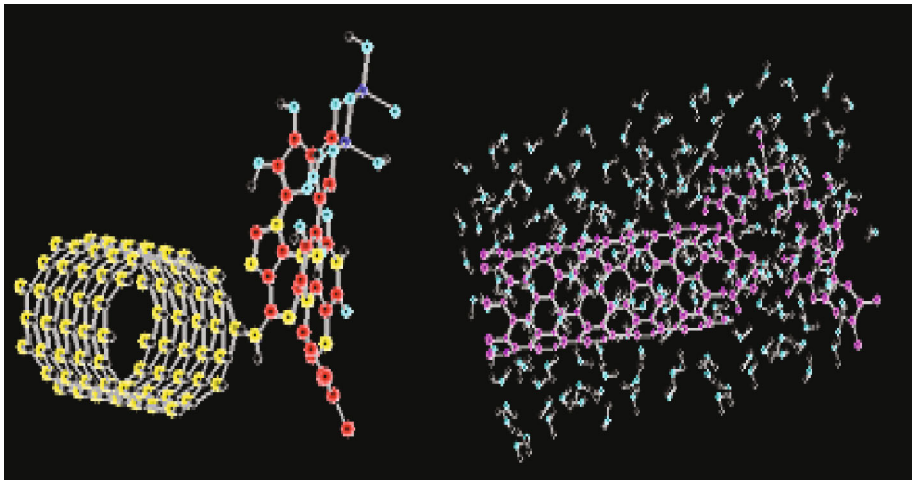

Fig. 1. Schematic depict of BNNT-FAD conjunction in water box.

with how the solution to multielectronic systems has been approached follows.

In this study, the geometries were optimized at the framework of DFT using the three-parameter Becke's exchange [45] and Lee–Yang–Parr's correlation nonlocal functional [46], usually known as BLYP and B3LYP method by 6-31G* basis set was used for description of electronic structure of (5, 5) single wall carbon nanotube (SWCNT) jointed to ancistroquinone using the NMR measurements on the basis of Gauge including atomic orbital (GIAO) [47].

In addition, the electrical conductivity of a solution of an electrolyte is measured by determining the resistance of the solution [48, 49].

An alternating voltage is used in order to avoid electrolysis. The resistance is measured by a conductivity meter. Typical frequencies used are in the range 1–3 kHz. The dependence on the frequency is usually small [50], but may become appreciable at very high frequencies, an effect known as the Debye–Falkenhagen effect.

In this paper, the Onsager model has been applied that was developed by Frisch, Wong, and Wiberg utilizes spherical cavities. Even though this implies a less accurate description of the solute and solvent interface, this approximation facilitates the evaluation of energy derivatives in geometry optimizations and frequency analysis. In addition, Cramer and Truhlar expanded this model at dipole level [51–55].

As a general rule, a cavity should have a physical meaning, such as that introduced by Onsager, and not be only a mathematical artifice as often happens in other descriptions of solvent effects [56]. On the physical meaning of Onsager's cavity, see also the comments. In particular, the cavity should exclude the solvent and contain within its boundaries the largest possible part of the solute charge distribution [56].

Quantum partial charges, accounting for polarization of the nanotube due to the weak ionic and covalent bonding of B–N and the polarization of the nanotube because of nanotube water interaction Jointed to FAD quenzyme extracted from glucose oxidase were computed by density functional theory (DFT) calculations. Gaussian 03 [57] was used for the HF and DFT calculations with B1LYP/B3LYP/6-31G** on the geometry-optimized structures. The partial charges on the tubes were obtained by fitting the electrostatic potential to fixed charges on the boron, nitrogen, and hydrogen atoms for the nanotube-biomaterial hybrid system (BNNT-FAD) linkage [58, 59].

The quantum partial charges are included in the calculation that the BNNT was jointed to FAD and water reservoirs are attached to the nanotube (Fig. 1).

RESULTS AND DISCUSSION

We first modeled a BNNT single-module fuel cell, applying FAD as the anode catalyst directly immobilized and then, the (5, 5) BNNT-FAD with water molecules was formed a single-file chain similar (Fig. 1). We then obtained geometry-optimized structure for BNNT-FAD method using Gaussian 03 [57].

The NMR data of isotropic (σ_{iso}), anisotropic shielding tensor (σ_{aniso}), chemical shift anisotropy ($\Delta\sigma$), chemical shift (δ), asymmetry (η) (ppm) have been reported for (5, 5) single wall boron nitride nanotube jointed to FAD vs. different atoms in Table 1 in water solvent.

Moreover, the influence of the solvent on the relative stability of our molecule was studied by means of the Onsager approach has been considered. The formations of hydrogen bonds between the confined water and nitrogen atoms on the BNNT can markedly

Table 1. Calculated electronic properties of BNNT-FAD complex in water box (NMR data in ppm)

Electronic parameters	N16	N21	B25	B24	H22	C11	N17	C6	N26	N27
					HF					
σ_{iso}	222.19	209.31	73.35	77.0444	33.16	185.98	281.53	200.93	167.04	185.12
σ_{aniso}	120.75	41.26	85.13	50.49	12.44	52.92	85.18	25.94	101.31	256.50
$\Delta\sigma$	120.74	41.26	−69.43	−73.70	−20.04	52.92	85.18	−37.20	101.31	107.06
δ	80.50	27.51	46.29	49.13	13.36	32.28	56.79	24.80	67.54	71.37
η	0.13	0.60	−0.36	−0.37	−0.24	0.75	0.30	−0.39	0.91	0.94
Atomic charge	−0.65	−0.76	0.82	0.77	0.33	0.54	−0.94	−0.05	−0.79	−0.79
					B1LYP					
σ_{iso}	246.65	232.61	76.07	66.96	32.39	199.95	305.28	215.20	185.87	201.94
σ_{aniso}	103.09	37.93	79.45	50.35	16.25	44.12	82.66	29.28	16.59	28.22
$\Delta\sigma$	103.09	37.93	−91.06	−63.19	−20.71	44.12	82.67	−30.54	−21.75	28.22
δ	68.73	25.28	60.70	42.12	13.81	29.41	55.11	20.36	14.50	18.79
η	0.11	0.86	−0.74	−0.59	−0.57	0.93	0.17	−0.91	−0.52	0.76
Atomic charge	−0.23	−0.28	0.35	0.31	0.20	0.10	−0.33	0.04	−0.37	−0.37
					B3LYP					
σ_{iso}	256.86	241.06	73.35	62.96	32.84	205.85	315.15	219.81	192.03	208.46
σ_{aniso}	109.62	37.28	85.13	85.13	17.10	45.18	87.53	29.92	10.20	23.85
$\Delta\sigma$	109.61	37.28	−100.37	−78.12	−21.53	45.18	87.53	−32.87	−19.10	−24.85
δ	73.08	24.85	66.92	52.08	14.35	30.12	58.35	21.92	12.73	16.57
η	0.17	0.91	−0.69	−0.49	−0.59	0.72	0.18	−0.82	−0.06	−0.92
Atomic charge	−0.24	−0.29	0.38	0.33	0.20	0.11	−0.35	−0.05	−0.39	−0.39

influence the structure and dynamical properties of water inside the tube (Fig. 2).

In addition, we have found that the isotropic and anisotropy shielding increase with the occupancy and consequently the negative charge (Figs. 2a, 2b).

Boron nitride nanotubes (BNNTs) have been reported to possess superior water permeation properties.

To investigate the effect of water molecules on the FAD-BNNT partial charges, we performed DFT calculations based on four different representative temperatures and levels of theory (HF, BLYP, and B3LYP). Due to the inhomogeneous distribution of water molecules along the tube axial direction, the partial charge distribution is not quite symmetric with respect to the center of the nanotube (Table 1 and Fig. 3).

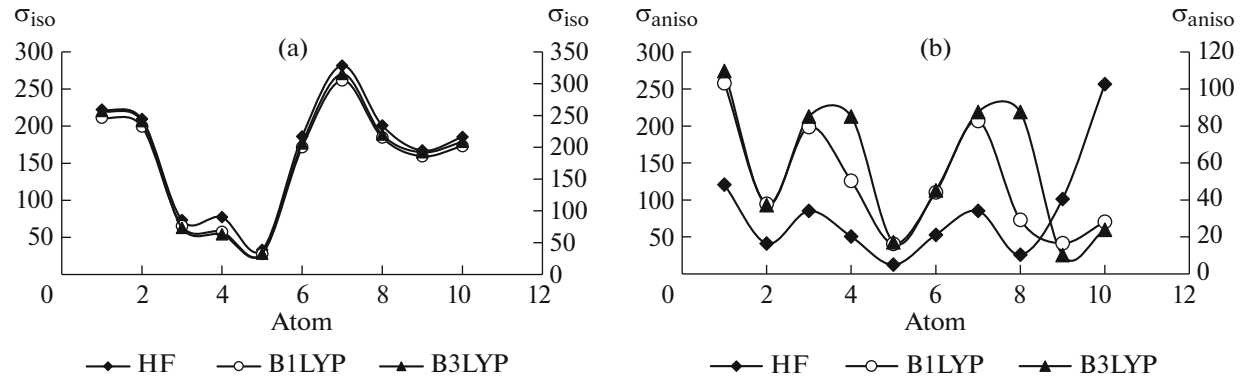

Fig. 2. The NMR plot of (a) isotropic (σ_{iso}), (b) anisotropic shielding tensor (σ_{aniso}) data in different levels of theory and 6-31G* basis set.

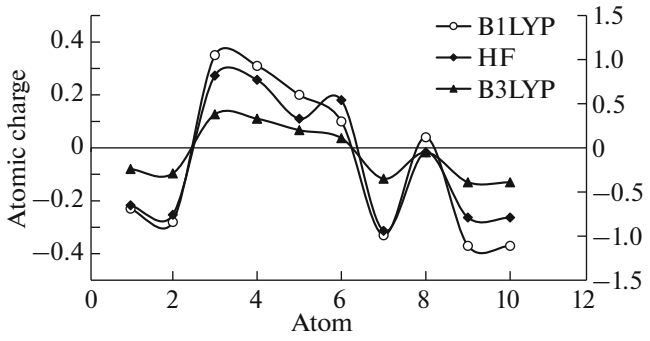

Fig. 3. Plot of the atomic charge data versus some active atoms of FAD in binding to BNNT to construct a biofuel cell based on electron transfer.

Electrolyte solutions are normally formed when a salt is placed into a solvent such as water and the individual components dissociate due to the thermodynamic interactions between solvent and solute molecules, in a process called solvation. Then we measured the atomic charge of some active atoms of FAD in binding to BNNT in water medium to form a multimodule biofuel cell based on the direct electron transfer principle (Fig. 3).

In this study thermo dynamic properties of BNNT and FAD and hybrid system were investigated respectively, next we examine the modification of temperature in water on this structure.

Results illustrated hybrid system has minimal level of free energy into FAD and BNNT (Table 2).

Boron nitride nanotube, because of its superior electrical, physical, and chemical properties has been considered such a fuel cell. Electron transfer between BNNT and FAD as a biofuel cell has the potential to operate close to thermodynamic redox potentials of the FAD active sites, thereby maximizing voltage output (Tables 2 and 3).

The voltage and current generated by the cell between the two BNNT and FAD were measured by resistance of water molecules for the voltage and current measurements (Fig. 4).

Table 3 showed the voltage-current and behaviors of the constructed BNNT-FAD fuel cell using theoretical methods with linear regressions of 0.9966 at 295, 298, 300, and 305 K (Fig. 4a).

In addition, it has been seen that by increasing the temperature, the resistance will be enhanced with linear correlation of 0.9807 (Fig. 4b).

The conductivity of a proton solution is a measure of its ability to electricity. Conductivity measurements are used routinely in many industrial and environmental applications as a fast, inexpensive and reliable way of measuring the ionic content in a solution [60].

Thus, the electrical conductivity of our electrolyte (BNNT-FAD in water box) has been measured by determining the resistance of the system (Fig. 5).

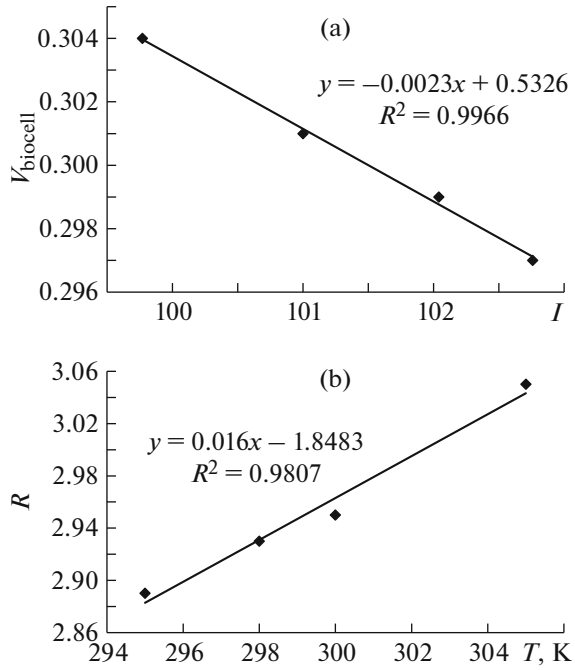

Fig. 4. Plot of (a) voltage–current behavior and (b) resistance–temperature of BNNT-FAD fuel cell using theoretical methods at 295, 298, 300, and 305 K.

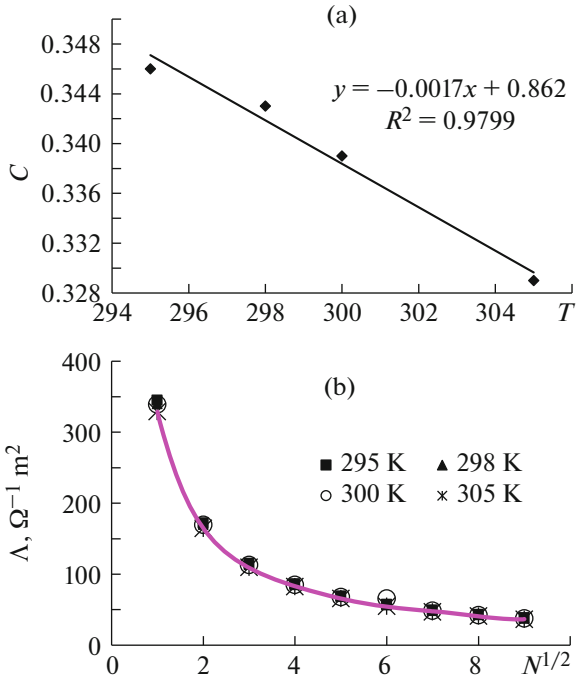

Fig. 5. Plot of (a) the electrical conductivity and (b) limiting ion conductivity of the BNNT-FAD in water box model in different temperatures and concentrations.

Table 2. Thermodynamic redox potentials of the FAD active site bonded to BNNT as a biofuel cell

Thermochemical properties	ΔH, HF				ΔS, cal/(K mol)				ΔG, HF			
method	T, K											
	295	298	300	305	295	298	300	305	295	298	300	305
HF	−1092.59	−1092.59	−1092.59	−1092.59	122.95	123.60	123.98	125.01	−1092.60	−1092.61	−1092.63	−1092.65
B1LYP	−1093.07	−1093.07	−1093.07	−1093.07	120.17	120.80	121.17	122.17	−1093.11	−1093.13	−1093.14	−1093.16
B3LYP	−1093.07	−1093.07	−1093.07	−1093.07	120.51	121.14	121.51	122.51	−1093.13	−1093.15	−1093.17	−1093.18

Table 3. Electrophysical parameters of BNNT-FAD biofuel cell at different temperatures in water box model

T, K	Method	$\Delta G \times 10^{-2}$, J	$E_{biocell}$, V	$K_{th} \times 10^{-4}$	Λ, S m^2 mol^{-1}	C, S	$R \times 10^3$, Ω	I, A	Power, W
295	HF	−286.58	0.297	11.87	344.57	0.344	2.90	102.41	30.41
	B1LYP	−286.63	0.297	11.89	344.92	0.346	2.89	102.77	30.52
	B3LYP	−286.69	0.297	11.92	345.34	0.346	2.89	102.76	30.56
298	HF	−288.34	0.299	11.33	336.63	0.336	2.97	100.60	30.05
	B1LYP	−288.56	0.299	11.43	338.13	0.339	2.95	101.36	30.30
	B3LYP	−288.91	0.299	11.59	340.53	0.341	2.93	102.04	30.26
300	HF	−290.52	0.301	11.44	338.29	0.339	2.95	102.05	30.72
	B1LYP	−290.61	0.301	11.48	338.90	0.339	2.95	102.03	30.72
	B3LYP	−290.73	0.301	11.54	339.71	0.340	2.94	102.47	30.87
305	HF	−293.67	0.304	10.70	327.19	0.327	3.05	99.77	30.36
	B1LYP	−293.84	0.304	10.77	328.29	0.329	3.04	100.16	30.49
	B3LYP	−293.92	0.304	10.81	328.80	0.329	3.04	100.19	30.51

In Fig. 5a, it has been demonstrated that with enhancing the temperatures, the electrical conductivity has be decreased.

Conductivity is traditionally determined by measuring the AC resistance of the solution between two electrodes. Dilute solutions follow Kohlrausch's laws of concentration dependence and additive of ionic contributions. Lars Onsager gave a theoretical explanation of Kohlrausch's law by extending Debye–Hückel theory (Fig. 5b).

Limiting ion conductivity for cation H^+ (λ_+^0) and anion OH^- (λ_-^0) in water at 298 K are 34.96, 19.91 mS × m^2 mol^{-1} [61].

In Fig. 5b, it has been obvious by increasing the square root of concentration ($N = 1 \times 10^{-4}$, 2×10^{-4}, 3×10^{-4}, 4×10^{-4}, 5×10^{-4}, 6×10^{-4}, 7×10^{-4}, 8×10^{-4}, 9×10^{-4} g-equiv), the limiting conductivity has been decreased in various temperatures.

With discussing the dependence of the power to resistance, a rapid decay in power generation was observed. This decrease might be due to combining BNNT to FAD complex (Fig. 6). The electric power generation demonstrated in this study clearly exhibited that biofuel cells employing FAD are capable of generating electric power utilizing variety of cellulolytic sugars as the substrate, including glucose. Consequently, we allowed utilizing cost effective and versatile boron nitride nanotube as the electrode materials in water environment in different temperatures.

Boron nanotube jointed to FAD immersed in an ionic solution has been studied extensively of applications in our biological–chemical system.

These results demonstrated that boron nitride nanotube is a feasible conductive material for the direct electron transfer type biofuel cell, for its potential cost efficiency, material flexibility and stability and the combination of FAD and BNNT will indicate

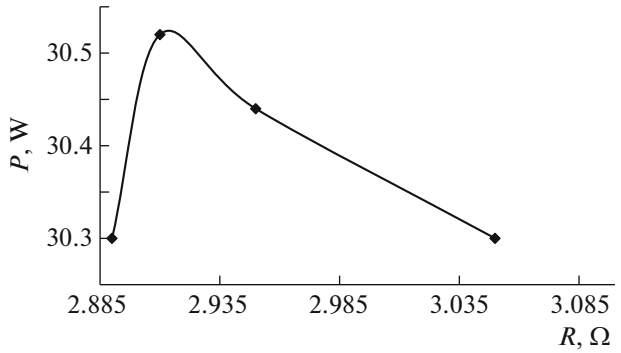

Fig. 6. Power generation from direct electron transfer type BNNT-FAD biofuel cell model.

the effective and practical electrochemical utilization of biofuel cell.

CONCLUSIONS

A biofuel cell has attracted much attention for generating electric power directly from sustainable fuel substrate. Thus, we have studied BNNT-FAD interaction by DFT and HF methods, and then we have investigated effects of BNNT-FAD as a hybrid system in order to optimize biofuel cell. Our result illustrated that BNNT can use effectively in biofuel cell.

Through considering different electron, with drawing of nitrogen atoms in BNNT jointed to FAD and analysis of NMR parameters it can be seen that the electron transferring caused more structural stability to BNNT-FAD complex because of hydrogen bonding in solution.

CONFLICT OF INTEREST

The authors declare that they have no conflicts of interest.

REFERENCES

1. E. Katz, B. Filanovsky, and I. Willner, New J. Chem. **23**, 481 (1999).
2. G. T. R. Palmore and G. M. Whitesides, in *Enzymatic Conversion of Biomass for Fuels Production,* Ed. by M. E. Himmel, J. O. Baker, and R. P. Overend, ACS Symp. Ser. **566**, 271 (1994).
3. R. A. Bullen, T. C. Arnot, J. B. Lakeman, and F. C. Walsh, Biosens. Bioelectron. **21**, 2015 (2006).
4. L. Zhang, S. Kang, and D. Kim, J. Comput. Theor. Nanosci. **10**, 1859 (2013).
5. V. W. Elloh, A. Yaya, A. K. Mishra, et al., Biointerface Res. Appl. Chem. **11**, 10864 (2021).
6. J. F. Rusling and Z. Zhang, in *Biomolecular Films,* Ed. by J. F. Rusling (Marcel Dekker, New York, 2003), p. 1.
7. V. Sharma, V. K. Vashistha, and D. K. Das, Biointerface Res. Appl. Chem. **11**, 7393 (2021).
8. J. F. Rusling and Z. Zhang, *Handbook of Surfaces and Interfaces of Mater,* Vol. 5 of *Biomolecules, Biointerfaces, and Applications,* Ed. by R. W. Nalwa (Academic, New York, 2001), Chap. 2, p. 10.
9. R. E. Renitta, V. D. Samuel, J. Patterson, et al., Biointerface Res. Appl. Chem. **11**, 7605 (2021).
10. S. C. Barton, J. Gallaway, and P. Atanassov, Chem. Rev. **104**, 4867 (2004).
11. Y. Degani and A. Heller, J. Phys. Chem. **91**, 1285 (1987).
12. Y. Degani and A. Heller, J. Am. Chem. Soc. **110**, 2615 (1988).
13. F. Barriere, P. Kavanagh, and D. Leech, Electrochim. Acta **51**, 5187 (2006).
14. H. M. Mustafa, G. Hayder, and A. H. Jagaba, Biointerface Res. Appl. Chem. **11**, 7431 (2021).
15. R. L. Fagan and B. A. Palfey, in *Comprehensive Natural Products II: Chemistry and Biology* (Elsevier, Amsterdam, 2010), Vol. 7, p. 37.
16. R. Teufel, A. Miyanaga, Q. Michaudel, et al., Nature (London, U. K.) **503** (7477), 552 (2013).
17. R. Teufel, F. Stull, M. J. Meehan, et al., J. Am. Chem. Soc. **137**, 8078 (2015).
18. W. Salaudden, I. Navabshan, and S. Banerjee, Biointerface Res. Appl. Chem. **11**, 14173 (2021).
19. M. Monajjemi, B. Honaparvar, B. K. Hadad, et al., African J. Pharm. Pharmacol. **4**, 521 (2010).
20. J. Liu, A. Chou, W. Rahmat, M. N. Paddon-Row, and J. J. Gooding, Electroanalysis **17**, 38 (2005).
21. S. N. Liu, Y. J. Yin, and C. X. Cai, Chin. J. Chem. **25**, 439 (2007).
22. S. Celasun, Rev. Theor. Sci. **1**, 319 (2013).
23. M. Tominaga, S. Nomura, and I. Taniguchi, Electrochem. Commun. **10**, 888 (2008).
24. R. A. Bullen, T. C. Arnot, J. B. Lakeman, and F. C. Walsh, Biosens. Bioelectron. **21**, 2015 (2006).
25. S. Konovalova and A. Avdeenko, Biointerface Res. Appl. Chem. **10**, 7070 (2020).
26. B. Ghalandari, M. Monajjemi, and F. Mollaamin, J. Comput. Theor. Nanosci. **8**, 1212 (2011).
27. F. Mollaamin, M. R. Gholami, H. Yoosbashizadeh, and S. K. Sadrnezhad, J. Phys. Theor. Chem. **1**, 19 (2004).
28. M. Monajjemi, L. Mahdavian, F. Mollaamin, and M. Khaleghian, Russ. J. Inorg. Chem. **54**, 1465 (2009).
29. D. Zhang and R. Q. Zhang, Chem. Phys. Lett. **371**, 426 (2003).
30. F. Mollaamin and M. Monajjemi, J. Comput. Theor. Nanosci. **12**, 1030 (2015).
31. V. S. Lee, P. Nimmanpipug, F. Mollaamin, et al., Russ. J. Phys. Chem A **83**, 2288 (2009).
32. E. M. Sarasia, S. Afsharnezhad, B. Honarparvar, et al., Phys. Chem. Liq. **49**, 561 (2011).
33. F. Barriere, P. Kavanagh, and D. Leech, Electrochim. Acta **51**, 5187 (2006).
34. Desriani, T. Hanashi, T. Yamazaki, et al., Open Electrochem. J. **2**, 6 (2010).
35. N. A. Al-Masoudi, R. S. Elias, and B. Saeed, Biointerface Res. Appl. Chem. **10**, 6444 (2020).
36. J. Okuda-Shimazaki, N. Kakehi, T. Yamazaki, et al., Biotechnol. Lett. **30**, 1753 (2008).

37. A. Tahan and F. Mollaamin, Russ. J. Phys. Chem. A **83**, 587 (2009).
38. A. M. Ilyin, Quantum Matter **2**, 205 (3013).
39. M. Monajjemi, M. Noei, and F. Mollaamin, Nucleotides Nucl. Acids **29**, 676 (2010).
40. M. Fizer, M. Slivka, and O. Fizer, Biointerface Res. Appl. Chem. **11**, 13885 (2021).
41. K. Bakhshi, F. Mollaamin, and M. Monajjemi, J. Comput. Theor. Nanosci. **8**, 763 (2011).
42. Q. Zhao, Rev. Theor. Sci. **1**, 83 (2013).
43. M. Khaleghian, M. Zahmatkesh, F. Mollaamin, and M. Monajjemi, Fullerenes, Nanotubes, Carbon Nanostruct. **19**, 251 (2011).
44. W. Koch and M. C. Holthausen, in *A Chemist's Guide to Density Functional Theory,* 2nd ed. (Wiley-VCH, Weinheim, 2000), pp. 3, 93.
45. A. D. Becke, J. Chem. Phys. **98**, 5648 (1993); A. D. Becke, Phys. Rev. A **38**, 3098 (1988).
46. C. Lee, W. Yang, and R. G. Parr, Phys. Rev. B **37**, 785 (1988); P. J. Stephens, F. J. Devlin, C. F. Chabalowski, and M. J. Frisch, J. Phys. Chem. **98**, 11623 (1994).
47. M. Monajjemi, S. Afsharnezhad, M. R. Jaafari, et al., Chemistry **17**, 55 (2008).
48. J. M. O'Bockris, A. K. N. Reddy, and M. Gamboa-Aldeco, *Modern Electrochemistry,* 2nd ed. (Springer, Berlin, 1998).
49. L. Buitrago, C. Ortiz, K. Barrientos, and M. Jaramillo, Biointerface Res. Appl. Chem. **10**, 5400 (2020).
50. M. Bešter-Rogač and D. Habe, Acta Chim. Slov. **53**, 391 (2006).
51. C. J. Cramer and D. G. Truhlar, J. Comput. Chem. **13**, 1089 (1992).
52. D. A. Liotard, G. D. Hawkins, G. C. Lynch, et al., J. Comput. Chem. **16**, 422 (1995).
53. C. C. Chambers, G. D. Hawkins, C. J. Cramer, and D. G. Truhlar, J. Phys. Chem. **100**, 16385 (1996).
54. D. J. Giesen, M. Z. Gu, C. J. Cramer, and D. G. Truhlar, J. Org. Chem. **61**, 8720 (1996).
55. L. J. Onsager, J. Am. Chem. Soc. **58**, 1486 (1936).
56. J. Tomasi, Theor. Chem. Acc. **103**, 196 (2000).
57. M. J. Frisch et al., *Gaussian 03, Rev. C.02* (Gaussian, Inc., Wallingford, CT, 2004).
58. F. Mollaamin, M. Monajjemi, S. Salemi, and M. T. Baei, Fullerenes, Nanotubes, Carbon Nanostruct. **19**, 182 (2011).
59. M. Monajjemi, M. T. Baie, and F. Mollaamin, Russ. Chem. Bull. **59**, 886 (2010).
60. J. R. Gray, in *Environmental Instrumentation and Analysis Handbook,* Ed. by R. D. Down and J. H. Lehr (Wiley, New York, 2004), p. 491.
61. M. R. Wright, *An Introduction to Aqueous Electrolyte Solutions* (Wiley, Chichester, 2007).